IEEE Access
Multidisciplinary ⋮ Rapid Review ⋮ Open Access Journal

Received January 25, 2022, accepted March 13, 2022, date of publication March 21, 2022, date of current version March 25, 2022.

Digital Object Identifier 10.1109/ACCESS.2022.3160835

Adaptive Neural Model Matching Control for Uncertain Immune Systems via H_∞ Approaches

YEONG-CHAN CHANG[1], HUI-MIN YEN[2], AND KUANG-FEN HAN[3]
[1]Department of Electrical Engineering, Kun Shan University, Tainan 710, Taiwan
[2]Green Energy Technology Research Center, Kun Shan University, Tainan 710, Taiwan
[3]Department of Nursing, Min-Hwei Junior College of Health Care Management, Tainan 736, Taiwan

Corresponding author: Hui-Min Yen (ec9526@mail.ksu.edu.tw)

This work was supported in part by the Green Energy Technology Research Center from the Featured Areas Research Center Program within the framework of the Higher Education Sprout Project by the Ministry of Education (MOE) in Taiwan, and in part by Kun Shan University under Grant 2020-109C04.

ABSTRACT The problem of the robust neural network-based model matching control is considered for a large class of uncertain immune systems. In order to achieve the purpose of therapeutic enhancement, it is essential to deal simultaneously with the effects of plant uncertainties, time-varying perturbations, and continuing environmental pathogens. Neural network control algorithm, robust H_∞ control theory and VSC technique are combined to construct the hybrid adaptive/robust tracking control scheme such that the controlled immune system achieves a satisfactory model matching control performance. An adaptive neural network system is constructed to learn the behavior of the immune system dynamics. Moreover, an algebraic Riccati-like inequality must be solved to achieve a desired H_∞ control performance. Consequently, the robust control scheme developed here can be analytically computed and easily implemented. Simulation results are presented to demonstrate the effectiveness of the proposed control scheme.

INDEX TERMS Immune systems, model matching, intelligent control scheme, disturbance attenuation, neural network system.

I. INTRODUCTION

The dynamic response of immune systems has received a significant research attention in past few decades [1]–[8]. The immune system is a rather complicated uncertain nonlinear system that may include a lot of uncertain infectious microorganisms (e.g., viruses, bacteria and parasites) and external environmental disturbances (e.g., continuing introduction of external pathogens). The main purpose of the immune control system is to effectively kill the invading microorganisms effectively, neutralize their response, provide the healing care for the affected organs, and protect the host against microbial infections. The mammalian immune system can be categorized into both the innate immune component and adaptive immune component. Medzhitov [9] proposed the recognition of microorganisms and activation of the immune response. His finding fully demonstrated two facts. First, the innate immune system consisted of functionally distinct modules that evolved to provide different forms of protection against pathogens. Second, the adaptive immune system could provide strategic response to invading microbe and yield protective cells.

For clinical treatment of infection, many models of immune response to infection have been proposed [10]–[13]. Furthermore, some control therapeutic methods of the immune response have been developed [3], [5], [14]–[22]. Hoshino *et al.* [3] investigated the immune response and biological behavior of quantum dots in vitro and in vivo, and concluded that all nanotechnology researchers should confirm the biological responses of their nanoscale products. Stengel *et al.* [5] presented a simple model for the response of the innate immune system and introduced a significant extension to the optimal control of enhancing immune response. Chang and Astolfi [14] proposed a control method of drug scheduling to enhance the response of immune system in an HIV model. Chien *et al.* [15] proposed a novel feedback linearization and almost disturbance decoupling method for the control of cancer immunotherapy on eliciting an immune system response against the tumor. Jiao *et al.* [16] proposed an adaptive control method for uncertain cancer-tumor-immune

The associate editor coordinating the review of this manuscript and approving it for publication was Hai Wang.

systems to track and stop the growth of cancer as well as maintain cancer and immune cells at an acceptable level. Maryam *et al.* [17] proposed an adaptive robust control for a second order nonlinear model of the interaction between cancer and immune cells of the body in order to control cancer growth and maintain the number of immune cells in an appropriate level. Dai and Liu [18] addressed an optimal control problem of a general reaction–diffusion tumor–immune system with chemotherapy to minimize the tumor burden and side effects as well as treatment costs in which the existence, uniqueness and some estimates of strong solution to the state system were obtained by making use of the semigroup theory and truncation method. Wong and Germain [19] addressed a robust control for the adaptive immune system which continually faced unpredictable circumstances yet reproducibly counteracted invading pathogens while limiting damage to self. The layered control schemes were employed to both buffers for exploiting different facets of cellular variation. McDaniel *et al.* [20] addressed the communication problem of a bi-directional flow of information between the innate immune system and adaptive immune system. They focused on how signals, first from pathogens and then from primed effector and memory T cells, were integrated by myeloid cells and its consequences for protective immunity or systemic inflammation. Abaricia *et al.* [21] reviewed the control of innate immune response by biomaterial surface topography, energy, and stiffness. They also highlighted recent advances of the role of innate immunity in response to implantable biomaterials as well as key mechanobiological findings in innate immune cells. Heiran *et al.* [22] developed a nonlinear adaptive control method to adjust the drug dose in renal transplant recipients with HCMV-infection. By using Lyapunov stability theorem the asymptotic stability of the closed-loop immune system was proved to guarantee the convergence of the system output to the desired scenario in the presence of different uncertainty levels.

In recent years, neural network systems have been successfully applied worldwide to universally approximate the mathematical models of dynamic systems [23], [24]. Chen *et al.* [24] proposed a RBF neural-network-based adaptive robust control design for nonlinear bilateral teleoperation manipulators with the communication time delay, various nonlinearities, and uncertainties. The slave environmental dynamics was modeled by a general RBF neural network, and its parameters were estimated and then transmitted for the environmental torque reconstruction in the master side. The trajectory creators in both of master and slave sides were applied to generate the desired trajectories, and the RBF-neural-network-based adaptive robust controller was proved to guarantee the global stability of bilateral teleoperation manipulators under time delay, and the good transparency performance was also achieved simultaneously. Several neural network- based control schemes were developed to treat the robust control of uncertain immune systems with various performance [25]–[28]. Moghtadaei *et al.* [25] proposed a variable structure fuzzy neural network model of squamous dysplasia and esophageal squamous cell carcinoma based on a global chaotic optimization algorithm. Khodaei-Mehr *et al.* [26] developed an intelligent optimal adaptive neuro-fuzzy controller to control the hepatitis C infection. In this population, a genetic algorithm was integrated to train the data that was utilized to build and train the Takagi-Sugeno fuzzy structure of the adaptive neuro-fuzzy inference system. The approximation error or external disturbance in these previous robust, adaptive or optimal control schemes [14]–[22], [25], [26] are assumed to be bounded. However, the external disturbance may be of finite-energy only, but not bounded. In this situation, the incorporation of an optimal H_∞ control scheme that possesses the capability of disturbance attenuation is necessary. Chen *et al.* [27] proposed a robust H_∞ model matching control of immune response for therapeutic enhancement to match a prescribed immune response. Chen *et al.* [28] proposed a robust H_∞ observer-based tracking control of stochastic immune response for a class of immune systems. By using the fuzzy approximation method, both the robust H_∞ model matching control and observer-based tracking control of immune systems could be solved via the linear matrix inequality technique. Here, in order to solve the min-imax control and the worst-case disturbance for the fuzzy dynamic game problem in [27] and [28], a complicated set of the Riccati-like inequalities must be solved. However, it is difficult to obtain a closed-form solution.

This paper addresses the problem of designing robust model matching controls for a large class of uncertain immune systems. A novel adaptive neural network-based model matching control design incorporated with a variable structure control (VSC) algorithm and a nonlinear H_∞ control algorithm is proposed. The results developed here possess the following enhancements:

1. This class of immune systems can be perturbed simultaneously by plant uncertainties, time-varying perturbations, and external environmental pathogens. Since measurement errors, modeling errors and process noises, etc. may appear in the practical immune system, the model of infectious disease described in this study exactly covers a very wide class of immune systems.
2. The neural network approximation system equipped with parameter updated law is designed to learn the behavior of the unknown dynamic functions. In turn an adaptive neural network-based dynamic feedback controller is developed such that all the states and signals of the closed-loop immune system are bounded and the model matching error can be made as small as possible.
3. The input weighting gains in all the pathogen killer's agent, immune cell enhancer, antibody enhancer, and organ health enhancer can be perturbed by small perturbations. In order to compensate the effects of these small perturbations, a modified algebraic Riccati- like inequality is solved to achieve the desired H_∞ control performance from the external disturbance to the model matching error. Therefore, the developed robust control

scheme not only can handle a large class of uncertain immune systems, but also achieve the aim of enhancing the stability performance.

4. A simple design procedure of the controller is summarized. Furthermore, a simple and explicit solution of the Riccati-like inequality can be exactly computed. Therefore, the intelligent robust control scheme developed here possesses the properties of computational simplicity and easy implementation from the viewpoint of practical applications.

This paper is organized as follows. In Section II, model descriptions are presented. Section III develops the intelligent adaptive/robust control scheme. Simulations are made in Section IV, and conclusions are given in Section V. In what follows, let $x : [0,\infty) \to R^n$ be in $L_2[0,\infty)$ if $\int_0^\infty x^T(t)x(t)\,dt < \infty$, and x be in $L_\infty[0,\infty)$ if $\|x(t)\| < \infty$. Let $\|A\|$ denote the induced 2-norm of matrix A. Let $A = diag\{a_1,\cdots,a_n\}$ be the diagonal matrix with diagonal elements a_i. Let $\Omega_{\hat{\theta}}$ be a preassigned constrained region of the estimated parameter $\hat{\Theta}(t)$, and let $\text{Proj}[\hat{\Theta}, f_\theta]$ denote the standard projection algorithm [23], [29].

II. MODEL DESCRIPTION AND PROBLEM FORMULATION

A. DESCRIPTION OF IMMUNE SYSTEMS

The dynamic model of infectious disease that is introduced to describe the change rates of pathogen, immune cell and antibody concentrations, and an indicator of organic health can be given by [5], [6], [27], [28]:

$$\begin{aligned}
\dot{x}_1 &= (a_{11} - a_{12}x_3)x_1 + b_1u_1 + d_1w_1\\
\dot{x}_2 &= a_{21}(x_4)a_{22}x_1x_3 - a_{23}(x_2 - x_2^*) + b_2u_2 + d_2w_2\\
\dot{x}_3 &= a_{31}x_2 - (a_{32} + a_{33}x_1)x_3 + b_3u_3 + d_3w_3\\
\dot{x}_4 &= a_{41}x_1 - a_{42}x_4 + b_4u_4 + d_4w_4\\
a_{21}(x_4) &= \begin{cases} \cos(\pi x_4), & 0 \le x_4 \le 1/2\\ 0, & 1/2 \le x_4 \end{cases}
\end{aligned} \tag{1}$$

where x_1, x_2 and x_3 are concentrations of a pathogen, immune cells and antibodies; x_4 is characteristic of damaged organ; u_1 is pathogen killer's agent; u_2, u_3 and u_4 are enhancers of immune cell, antibody and organ health; w_1 is rate of continuing introduction; w_2, w_3, w_4 are environmental disturbances; $a_{21}(x_4)$ is the mediation of immune cell generated by the damaged cell organ; b_1, b_2, b_3, b_4 are control input gains; and d_1, d_2, d_3, d_4 are coupling gains of environmental disturbances. The structural relationship of system variables is depicted in Fig. 1 [5], [6], [27], [28]. The mathematical model described in (1) is an idealization of a generic humoral immune response that subsumes many details into aggregated effects [30]. That is, the model presented in [30] does not account for any treatment. In contrast, the model in (1) has added idealized active and passive immunotherapeutic control agents $u_1,\cdots,u_4$ as well as an exogenous input $w_1,\cdots,w_4$ into the model. Active immunotherapy strengthens natural immune response, as by enhancing plasma cell and antibody production, while passive immunotherapy addresses the effects of infection directly, as in killing the pathogen or healing the infected organ [5], [6], [27], [28].

The dynamic immune response in (1) can be rewritten as in the following compact form:

$$\dot{x}(t) = f(x(t)) + Bu(t) + Dw(t) \tag{2}$$

where

$$\begin{aligned}
&x = [x_1, x_2, x_3, x_4]^T, \quad u = [u_1, u_2, u_3, u_4]^T,\\
&w = [w_1, w_2, w_3, w_4]^T, \quad B = diag\{b_1, b_2, b_3, b_4\},\\
&D = diag\{d_1, d_2, d_3, d_4\},\\
&f(x) = \begin{bmatrix} f_1(x)\\ f_2(x)\\ f_3(x)\\ f_4(x) \end{bmatrix} = \begin{bmatrix} (a_{11} - a_{12}x_3)x_1\\ a_{21}(x_4)a_{22}x_1x_3 - a_{23}(x_2 - x_2^*)\\ a_{31}x_2 - (a_{32} + a_{33}x_1)x_3\\ a_{41}x_1 - a_{42}x_4 \end{bmatrix}.
\end{aligned}$$

From the viewpoint of practical applications, the immune system may be involved with a lot of uncertain perturbations and continuing introduction of external pathogens. Here, in order to coincide with the practical situation and achieve the purpose of therapeutic enhancement, the nonlinear function $f(x)$ is assumed to be completed unknown and the input gains b_1, b_2, b_3, b_4 are assumed to be perturbed by time-varying uncertainties.

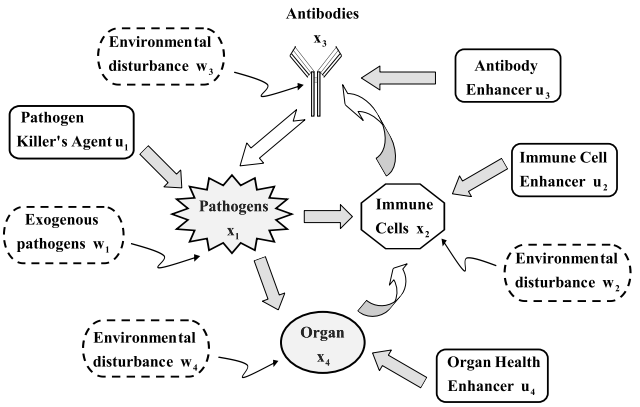

FIGURE 1. Innate and enhanced immune responses to a pathogenic attack by exogenous pathogens (w_1) involving with environmental disturbances (w_2, w_3, w_4), pathogen killer's agent (u_1) and control input enhancers (w_2, w_3, w_4).

B. PROBLEM FORMULATION

Give a desired reference model

$$\dot{x}_r(t) = A_r x_r(t) + r(t) \tag{3}$$

where $x_r(t)$ is reference state vector, A_r is asymptotically stable matrix, and $r(t)$ is desired reference signal. Define the matching error $e(t) = x(t) - x_r(t)$.

The objective of this paper is to construct intelligent adaptive model matching control scheme for the immune system described in (1) that may be simultaneously involved with the effects of plant uncertainties, time-varying perturbations, and continuing environmental pathogens, such that the states

and signals of the closed-loop controlled immune system remain bounded, the model matching control performance is achieved, and the effect due to the external disturbance on the matching error can be attenuated to any prescribed level, i.e. for a given desired attenuation $\rho > 0$ and a matrix $Q = Q^T > 0$, the following H_∞ criterion is achieved:

$$\int_0^T e^T(t)Qe(t)\,dt \le U_0 + \rho^2 \int_0^T w^T(t)w(t)dt \qquad (4)$$

where U_0 is a positive constant depending on the initial conditions.

C. DESCRIPTION OF NEURAL NETWORK SYSTEMS

Neural network systems possess the advantages of performance enhancement and learning capability by using parallel distributed processing. A simple two-layer neural network model shown in Fig. 2 is constructed in this study to learn the behavior of the unknown function $f_i(x)$, $i = 1, \cdots, 4$ whose basic configuration is implemented by using massive connections among processing units. The four inputs to this model are the concentrations of pathogen x_1, immune cells x_2, and antibodies x_3, and characteristic of damaged organ x_4. The output $y_i(\cdot)$, $i = 1, \cdots, 4$ can be given by [23]

$$y_i(x, \hat{\Theta}_i) = \sum_{l=1}^{m_i} \theta_{il} y_{il}\Big(\sum_{j=1}^{4} \omega_{ijl} x_j + b_{il}\Big), \quad i = 1, \cdots, 4 \qquad (5)$$

where m_i, $i = 1, \cdots, 4$ is the number of hidden neurons, $y_{il}(\cdot)$, $i = 1, \cdots, 4$, $l = 1, \cdots, m_i$ denotes the activation function, ω_{ijl}, $i, j = 1, \cdots, 4$, $l = 1, \cdots, m_i$ is the first-to-second layer interconnection weights, b_{il}, $i = 1, \cdots, 4$, $l = 1, \cdots, m_i$ is the biases, and θ_{il}, $i = 1, \cdots, 4$, $l = 1, \cdots, m_i$ is the second-to-output interconnection weights.

Universal approximation theorem [23]: the neural network system in the form of (5) is proven to be an universal approximator, i.e., for any given real continuous function $f_i(x)$ on the compact set Ω_x, there exists a neural network system $y_i(x, \hat{\Theta}_i)$ in the form of (5) such that it can uniformly approximate $f_i(x)$ over Ω_x to arbitrary accuracy.

III. DESIGN OF ROBUST THERAPEUTIC CONTROLLER

Taking into account the state equation (2) and the reference model (3), the dynamic equation of the matching error $e(t) = x(t) - x_r(t)$ can be computed as

$$\dot{e}(t) = A_r e(t) + f(x(t)) + Bu(t) + Dw(t) - A_r x(t) - r(t) \qquad (6)$$

In the practical immune system, the input weighting gains b_1, b_2, b_3, b_4 may have uncertain variations around their nominal values because of receiving unpredictable time-varying interference from the environment, etc. Here, in order to coincide with practical applications, these gains can be split into a known nominal part plus an unknown perturbation, i.e. $b_i = b_{i0} + \Delta b_i(t)$, $i = 1, \cdots, 4$. Let $B_0 = diag\{b_{10}, \cdots, b_{40}\}$ and $\Delta B(t) = diag\{\Delta b_1, \cdots, \Delta b_4\}$. We make the following assumption.

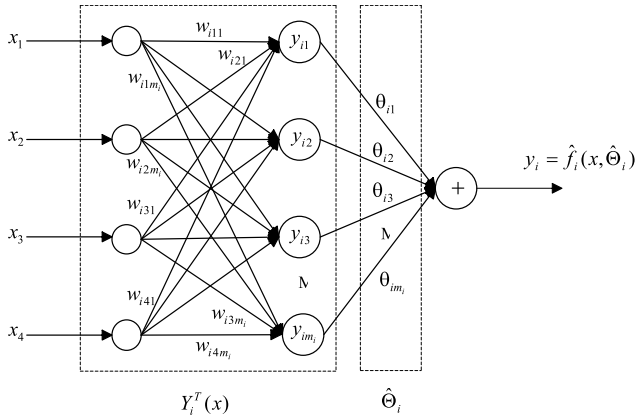

FIGURE 2. Basic configuration of the two-layer neural network system $\hat{f}_i(x, \hat{\Theta}_i)$, $i = 1, 2, 3, 4$ that is designed to learn the behavior of the unknown function $f_i(x)$, $i = 1, 2, 3, 4$.

A1: There is a positive function $0 \le \kappa_b(t) < 1$ such that $\left\| B_0^{-1} \Delta B \right\| \le \kappa_b(t)$. □

Moreover, an adaptive neural network approximation system $\hat{f}(x, \hat{\Theta})$ with input vector $x \in \Omega_x$ for some compact set Ω_x and the tunable approximation parameter vector $\hat{\Theta}$, is proposed here to approximate the behavior of the uncertain function $f(x)$. Let

$$\hat{f}(x, \hat{\Theta}) = [\hat{f}_1(x, \hat{\Theta}_1), \hat{f}_2(x, \hat{\Theta}_2), \hat{f}_3(x, \hat{\Theta}_3), \hat{f}_4(x, \hat{\Theta}_4)]^T \qquad (7)$$

where $\hat{f}_i(x, \hat{\Theta}_i)$, $i = 1, 2, 3, 4$ is designed to learn the ith component $f_i(x)$ of $f(x)$. As in many previous studies [23], [24], [27], [29], the linearly parametrized model is employed in the approximation procedure and so $\hat{f}_i(x, \hat{\Theta}_i)$ can be expressed as

$$\hat{f}_i(x, \hat{\Theta}_i) = Y_i^T(x)\hat{\Theta}_i \qquad (8)$$

where $\hat{\Theta}_i \equiv [\theta_{i1}, \cdots, \theta_{im_i}]^T$ and $Y_i(x) \equiv [y_{i1}, \cdots, y_{im_i}]^T$ for some $m_i > 0$ is a regressive vector with the regressor

$$y_{il}(x) = \frac{e^{\sigma_{il}(x)} - e^{\sigma_{il}(x)}}{e^{\sigma_{il}(x)} + e^{\sigma_{il}(x)}} \qquad (9)$$

for $i = 1, \cdots, 4$ and $l = 1, \cdots, m_i$.

Consequently, the total approximation system $\hat{f}(x, \hat{\Theta})$ can be expressed as

$$\hat{f}(x, \hat{\Theta}) = Y(x)\hat{\Theta} \qquad (10)$$

where $Y(x) = diag\{Y_1^T(x), Y_2^T(x), Y_3^T(x), Y_4^T(x)\}$ denotes a basis matrix and $\hat{\Theta} \equiv [\hat{\Theta}_1^T, \cdots, \hat{\Theta}_4^T]^T$. According to the universal approximation theorem [23], there is an optimal approximation parameter Θ^* such that $\hat{f}(x, \Theta^*)$ can approximate $f(x)$ as best as possible. Therefore, the unknown dynamics $f(x)$ can be expressed as

$$f(x) = Y(x)\Theta^* + \Delta f(x) \qquad (11)$$

where $\Delta f(x)$ denotes the optimal approximation error. The following assumption is made.

A2: There is a positive function $\kappa_f(x) \geq 0$ such that $\|\Delta f(x)\| \leq \kappa_f(x)$. □

Choose the control input

$$u = B_0^{-1}(-Y(x)\hat{\Theta} + A_r x + r) + u_{new} \tag{12}$$

for some new control input u_{new}. By taking into account (11), (12) and assumption A1, (6) can be expressed as:

$$\dot{e}(t) = A_r e + Y\tilde{\Theta} + \Delta f_e(x_e, t) + B_0(I + B_0^{-1}\Delta B)u_{new} + Dw \tag{13}$$

where $\Delta f_e(\cdot) = \Delta f + \Delta B B_0^{-1}(-Y\hat{\Theta} + A_r x + r)$, $\tilde{\Theta} = \Theta^* - \hat{\Theta}$, and $x_e = [x^T, \hat{\Theta}^T, r^T]^T$. Note that the uncertain term $\Delta f_e(\cdot)$ is yielded due to the small perturbation, $\Delta B(t)$, and the approximation error, $\Delta f(x)$, and so this term can be omitted when these two terms are equal to zero. A VSC algorithm is employed to override the effect of uncertain term $\Delta f_e(x_e, t)$. According to the assumptions A1 and A2, there is a positive function $M_s(x_e, t) > 0$ such that $\|\Delta f_e(x_e, t)\| \leq M_s(x_e, t)$.

Theorem 1: Consider the uncertain immune systems (1). Suppose assumptions A1 and A2 hold. Then, if there exists a matrix $P = P^T \geq 0$ satisfying the following Riccati-like inequality

$$\frac{1}{2}(PA_r + A_r^T P) + \frac{1}{4\rho^2}PDD^T P - PB_0\frac{1-\kappa_b}{r_h}B_0^T P + Q \leq 0 \tag{14}$$

for some H_∞ control gain $r_h > 0$, the robust-adaptive neural network-based model matching control law

$$u(t) = B_0^{-1}(-Y(x)\hat{\Theta} + A_r x + r) + u_h(t) + u_s(t) \tag{15}$$

$$u_h(t) = -\frac{1}{r_h}B_0^T Pe \tag{16}$$

$$u_s(t) = -B_0^{-1}\frac{M_s(x_e, t)}{1-\kappa_b(t)}\frac{M_s(x_e, t)B_0^T Pe}{\|M_s(x_e, t)B_0^T Pe\| + \varepsilon e^{-\nu t}} \tag{17}$$

$$\dot{\hat{\Theta}} = \gamma\,\mathrm{Proj}\,[\hat{\Theta}, Y^T(x)Pe] \tag{18}$$

where $\varepsilon > 0$, $\nu > 0$ are constants and $\gamma > 0$ is the adaptive gain, guarantees that

(i) if $w \in L_2[0, \infty)$, then the following H_∞ performance is achieved:

$$\int_0^T e^T(t)Qe(t)\,dt \leq \frac{1}{2}e^T(0)Pe(0) + \frac{1}{2\gamma}\tilde{\Theta}^T(0)\tilde{\Theta}(0) + \rho^2\int_0^T w^T(t)w(t)dt + \frac{\varepsilon}{\nu}(1 - e^{-\nu T}) \tag{19}$$

(ii) if $w \in L_\infty[0, \infty)$, then the matching error can be made as small as possible; and (iii) all the states and signals are bounded.

Proof: Choose the Lyapunov function

$$U(e, \tilde{\Theta}, t) = \frac{1}{2}e^T Pe + \frac{1}{2\gamma}\tilde{\Theta}^T\tilde{\Theta} \tag{20}$$

Taking into account (13), the derivative of U is

$$\dot{U} = \frac{1}{2}e^T PA_r e + \frac{1}{2}e^T A_r^T Pe + e^T P\Delta f_e(x_e, t) + e^T PDw + e^T PB_0(I + B_0^{-1}\Delta B)(u_h + u_s) + e^T PY(x)\tilde{\Theta} - \frac{1}{\gamma}\dot{\hat{\Theta}}^T\tilde{\Theta} \tag{21}$$

By completing the squares, we get

$$e^T PDw \leq \frac{1}{4\rho^2}e^T PDD^T Pe + \rho^2 w^T w \tag{22}$$

From assumption A1, we get

$$e^T PB_0\frac{1-\kappa_b}{r_h}B_0^T Pe \leq e^T PB_0\frac{I + B_0^{-1}\Delta B}{r_h}B_0^T Pe \tag{23}$$

Substituting (16), (22) and (23) into (21) yields

$$\dot{U} \leq \frac{1}{2}e^T PA_r e + \frac{1}{2}e^T A_r^T Pe + \frac{1}{4\rho^2}e^T PDD^T Pe + \rho^2 w^T w - e^T PB_0\frac{1-\kappa_b}{r_h}B_0^T Pe + e^T P\Delta f_e(x_e, t) + e^T PB_0(I + B_0^{-1}\Delta B)u_s + e^T PY(x)\tilde{\Theta} - \frac{1}{\gamma}\dot{\hat{\Theta}}^T\tilde{\Theta} \tag{24}$$

Substituting (14) into (24) leads to

$$\dot{U} \leq -e^T Qe + \rho^2 w^T w + e^T P\Delta f_e(x_e, t) + e^T PB_0(I + B_0^{-1}\Delta B)u_s + e^T PY(x)\tilde{\Theta} - \frac{1}{\gamma}\dot{\hat{\Theta}}^T\tilde{\Theta} \tag{25}$$

From (18) that is a standard projection algorithm [23], [29], it is clear that $\hat{\Theta}(t) \in \Omega_{\hat{\theta}}$ for all $t \geq 0$, and

$$e^T PY(x)\tilde{\Theta} - \frac{1}{\gamma}\dot{\hat{\Theta}}^T\tilde{\Theta} \leq 0. \tag{26}$$

Moreover, from $u_s(t)$ in (17) and the definition of $M_s(\cdot)$, we get

$$e^T PB_0(I + B_0^{-1}\Delta B)u_s + e^T P\Delta f_e(x_e, t) \leq \varepsilon e^{-\nu t} \tag{27}$$

Substituting (26) and (27) into (25) yields

$$\dot{U}(e, \tilde{\Theta}, t) \leq -e^T Qe + \rho^2 w^T w + \varepsilon e^{-\nu t} \tag{28}$$

(i) Suppose $w \in L_2[0, \infty)$, i.e., there is a $M_d > 0$ such that $\int_0^\infty \|w(t)\|^2 dt < M_d$. Integrating the inequality (28) from 0 to T achieves the H_∞ performance in (19). Moreover, integrating (28) yields $U(t) \leq U(0) + \rho^2 M_d + \varepsilon/\nu \equiv U_{\max}$ for all $t \geq 0$. From (20) we can conclude $e(t) \in \{e|\ e^T Pe \leq 2U_{\max}\}$ and $\tilde{\Theta}(t) \in \{\tilde{\Theta}|\ \tilde{\Theta}^T\tilde{\Theta} \leq 2\gamma U_{\max}\}$. This implies all the states and signals are bounded.

(ii) Suppose $w \in L_\infty[0, \infty)$, i.e., there is an $\varepsilon_w > 0$ such that $\|w\| \leq \varepsilon_w$. From (28), we obtain $\dot{U} \leq -\lambda_q\|e\|^2 + \varepsilon_\infty$ where λ_q denotes the minimum eigenvalue of Q and $\varepsilon_\infty = \rho^2\varepsilon_w^2 + \varepsilon$. If we choose $\lambda_q > \varepsilon_\infty/\mu^2$ for some small value $\mu > 0$, then there is a $\xi > 0$ such that

$$\dot{U} \leq -\xi\|e\|^2 < 0 \tag{29}$$

for all $\|e\| > \mu$. This implies there is a $T > 0$ such that $\|e(t)\| \leq \mu$ for all $t \geq T$, that is the UUB tracking performance is achieved [31]. □

Remark 1: i) The intelligent neural network-based robust controller structure (14)-(18) is depicted in Fig. 3 that consists of three parts: an adaptive approximation system $Y(x)\hat{\Theta}$ equipped with (18) is designed to learn the behavior of $f(x)$, the robust H_∞ controller u_h is used to achieve the desired H_∞ performance, and the VSC scheme u_s is used to eliminate the effect of $\Delta f_e(x_e, t)$ Hence, in practice this controller is a hybrid adaptive-robust controller.

ii) The control design relies on the solution of an algebraic Riccati-like matrix inequality in (14). A simple solution of (14) can be computed as follows. Choose the robust H_∞ control gain, r_h such that

$$\frac{1}{4\rho^2}DD^T - B_0\frac{1-\kappa_b}{r_h}B_0^T \le 0 \tag{30}$$

and so (14) is reduced to $PA_r + A_r^T P + 2Q \le 0$ that is the Lyapunov inequality. Since A_r is a Hurwitz matrix, for any given positive definite symmetric matrix Q, $PA_r + A_r^T P + 2Q = 0$ has the unique solution

$$P = 2\int_0^\infty \exp(A_r^T t)Q\exp(A_r t)\,dt[31].$$

(iii) A simple design procedure of implementing the matching controller developed in Theorem 1 is summarized as follows:

Step 1: Give a desired model $\dot{x}_r(t) = A_r x_r(t) + r(t)$.

Step 2: Construct the adaptive neural network approximation system $\hat{f}(x, \hat{\Theta})$.

Step 3: Give a desired attenuation level $\rho > 0$ and a matrix $Q = Q^T > 0$.

Step 4: Choose the H_∞ control gain, r_h, in (30).

Step 5: Solve the Riccati-like inequality $PA_r + A_r^T P + 2Q \le 0$ to obtain the matrix P.

Step 6: Construct the adaptive neural network-based model matching controller (15)-(18). □

The term $\frac{\varepsilon}{\nu}(1 - e^{-\nu T})$ in (19) is yielded owing to the smooth modification of $u_s(t)$ and can be viewed as an external disturbance. It is clear that the smaller the value ε and the larger the value ν, the less smooth is the robust controller $u_s(t)$ and the smaller is the term $\frac{\varepsilon}{\nu}(1 - e^{-\nu T})$. It is noted that the VSC scheme u_s in (17) is used to eliminate the effect of $\Delta f_e(x_e, t)$. If $\Delta f_e(x_e, t) = 0$, then the VSC scheme can be omitted, and a standard H_∞ performance can be concluded.

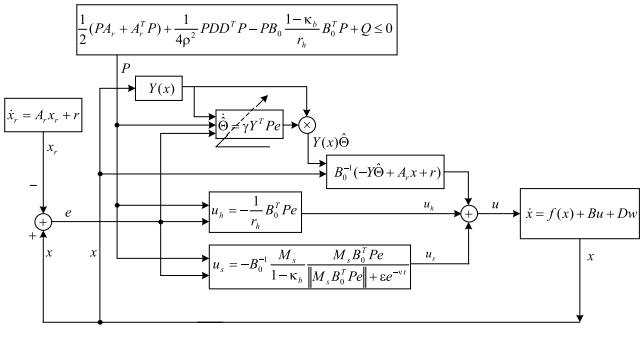

FIGURE 3. Block diagram of the intelligent adaptive neural network-based model matching control structure for the immune system developed in Theorem 1. This controller structure consists of three parts. The first part is an intelligent adaptive approximation system $Y(x)\hat{\Theta}$ equipped with update law (18), the second part is the robust H_∞ controller u_h in (16), and the third part is the VSC scheme u_s in (17).

Corollary 1: Consider the uncertain immune systems (1). Suppose $\Delta f_e(\cdot) = 0$. Then, if there exists a matrix $P = P^T \ge 0$ satisfying (14), the robust-adaptive neural network-based model matching control law (15)-(18) with $u_s(t) = 0$ guarantees that the following H_∞ performance is achieved:

$$\int_0^T e^T(t)Qe(t)\,dt \le U(0) + \rho^2\int_0^T w^T(t)w(t)dt \tag{31}$$

Proof: Choose the Lyapunov function as in (20). Taking the similar procedure of proof in Theorem 1, the derivative of U can be bounded as

$$\dot{U}(e, \tilde{\Theta}, t) \le -e^T Qe + \rho^2 w^T w \tag{32}$$

Integrating the inequality (32) from 0 to T yields the H_∞ performance (31). □

IV. SIMULATION EXAMPLE

Consider the innate immune system (1) shown in Figure 1. For the purpose of simulation, the system function in (2) is given by $f(x) = [(1 - x_3)x_1,\ 3a_{21}(x_4)x_1x_3 - (x_2 - 2),\ x_2 - (1.5 + x_1)x_3,\ 0.5x_1 - x_4]^T$, $B_0 = diag\{-1, -1, 1, -1\}$, $D = diag\{1, 1, 1, 1\}$. The exact parameter values are described in Table 1. Since time-varying perturbations and disturbances noises may be yielded due to measurement errors, modeling errors and process noises [4], the nonlinear function $f(x)$ is completed unknown, i.e. the coefficients a_{ij} for $i, j = 1, \cdots, 4$ are not required in the implementation of control design. Moreover, the input gains b_1, b_2, b_3, and b_4 are perturbed by $\Delta b_1 = 0.1\sin(t)$, $\Delta b_2 = 0.1\cos(t)$, $\Delta b_3 = 0.15\sin(0.5t)$, $\Delta b_4 = 0.12\cos(0.5t)$, respectively. The external disturbances w_1, w_2, w_3, and w_4 are assumed to be zero mean white noises with standard deviations 0.3. Adopting the above parameters, the dynamic model of the innate immune system perturbed by plant uncertainties, time-varying perturbations, and external environmental pathogens can be expressed as

$$\begin{aligned}
\dot{x}_1 &= (1 - x_3)x_1 - (1 + 0.1\sin t)u_1 + w_1\\
\dot{x}_2 &= 3a_{21}(x_4)x_1x_3 - (x_2 - 2) - (1 + 0.1\cos t)u_2 + w_2\\
\dot{x}_3 &= x_2 - (1.5 + x_1)x_3 + (1 + 0.15\sin 0.5t)u_3 + w_3\\
\dot{x}_4 &= 0.5x_1 - x_4 - (1 + 0.12\cos 0.5t)u_4 + w_4
\end{aligned}$$

For the purpose of comparison, the simulation results of the lethal case of the uncontrolled innate immune response without the presence of environmental disturbances (i.e., let $u_i = 0$ and $w_i = 0$, $i = 1, \cdots, 4$) are shown in Fig. 4 with the initial state $x(0) = [3,\ 3.1,\ 1,\ 1]^T$. The simulations are performed in the MATLAB environment and the corresponding programs are provided in the Appendix A. One can see that this uncontrolled response is quite poor. The pathogen concentration (x_1, black, solid line) is increasing rapidly and causes organ failure (x_4, green, dotted line).

The robust-adaptive neural network-based model matching controller (15)-(18) with the desired H_∞ performance (19) is employed to treat the model matching control problem. According the design algorithm in Remark 1-(iii), the implementation of the matching controller from step 1 to step 6 is described as follows.

Step 1: Our reference model design objective is that system matrix A_r and $r(t)$ should be specified beforehand so that its transient response and steady state of reference system for innate immune response system are desired. Here, for the purpose of simulation, let the desired signal $x_r = [x_{r1}, x_{r2}, x_{r3}, x_{r4}]^T$ be specified by $A_r = diag\{-1.1, -2, -4, -1.5\}$ and $r(t) = [0,\ 4,\ 16/3,\ 0]^T u_{step}(t)$ where $u_{step}(t)$ is the unit step function. The initial condition is set as $x_r(0) = [2.9,\ 3.2,\ 1.1,\ 1.05]^T$. After some manipulations, the desired reference trajectories are obtained as $x_{r1}(t) = 2.9e^{-1.1t}$, $x_{r2}(t) = 1.2e^{-2t} + 2$, $x_{r3}(t) = -0.23e^{-4t} + 1.33$, and $x_{r4}(t) = 1.05e^{-1.5t}$, respectively. The time responses of $x_r(t)$ are depicted in Fig. 5. The corresponding programs are provided in the Appendix B. These simulation results show that the desired trajectory $x_{r1}(t)$ of the pathogen concentration $x_1(t)$ exponentially converges to zero with exponential rate -1.1, the desired trajectory $x_{r2}(t)$ of the immune cell concentration $x_2(t)$ exponentially converges to 2 with exponential rate -2, the desired trajectory $x_{r3}(t)$ of the antibody concentration $x_3(t)$ exponentially converges to 1.33 with exponential rate -4, and the desired trajectory $x_{r4}(t)$ of the organ characteristic $x_4(t)$ exponentially converges to zero with exponential rate -1.5. The exponential rates are dependent on the eigenvalues of A_r. If the eigenvalues are more negative (i.e. more robust stable), the tracking system will be more robust to environmental disturbances. The exponentially convergent values are dependent on the values of $r(t)$ and A_r.

TABLE 1. Model parameters of the immune system [5], [6].

Symbol	Description	Value
a_{11}	Pathogens reproduction rate coefficient	1
a_{12}	The suppression by pathogens rate coefficient	1
a_{22}	Immune reactivity coefficient	3
a_{23}	The mean immune cell production rate coefficient	1
x_2^*	The steady-state concentration of immune cells	2
a_{31}	Pathogens reproduction rate coefficient	1
a_{32}	The antibody mortality coefficient	1.5
a_{33}	The rate of antibodies suppress pathogens	1
a_{41}	The organ damage depends on the pathogen damage possibilities coefficient	0.5
a_{42}	Organ recovery rate	1
b_1	Pathogen killer's agent coefficient	-1
b_2	Immune cell enhancer coefficient	-1
b_3	Antibody enhancer coefficient	1
b_4	Organ health enhancer coefficient	-1
d_1	Coupling gains of disturbance w_1	1
d_2	Coupling gains of disturbance w_2	1
d_3	Coupling gains of disturbance w_3	1
d_4	Coupling gains of disturbance w_4	1

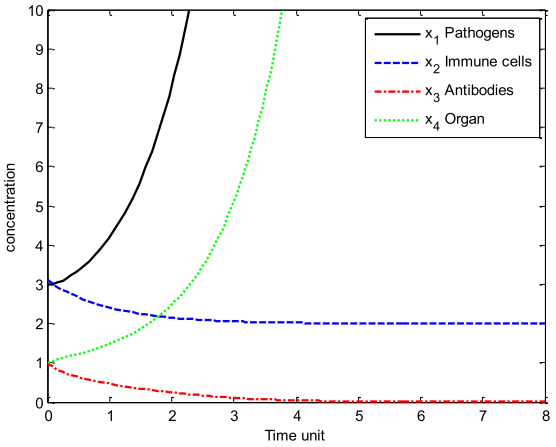

FIGURE 4. The uncontrolled immune response in (1) with $u_1 = u_2 = u_3 = u_4 = 0$, $w_1 = w_2 = w_3 = w_4 = 0$. The initial conditions of the immune system are $x(0) = [3,\ 3.1,\ 1,\ 1]^T$.

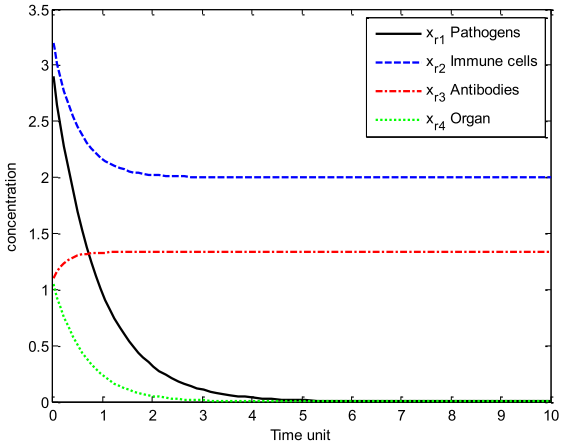

FIGURE 5. The time response of the desired reference model in (3) with $x_r(0) = [2.9,\ 3.2,\ 1.1,\ 1.05]^T$.

Step 2: Choose the activation functions of the adaptive neural network system $\hat{f}(x, \hat{\Theta})$ as

$$y_{1i} = \frac{e^{5(x_1-0.5i)} - e^{-5(x_1-0.5i)}}{e^{5(x_1-0.5i)} + e^{-5(x_1-0.5i)}}, \quad i = 1, 2, 3$$

$$y_{2i} = \frac{e^{5(x_2-1-0.5i)} - e^{-5(x_2-1-0.5i)}}{e^{5(x_2-1-0.5i)} + e^{-5(x_2-1-0.5i)}}, \quad i = 1, 2, 3$$

$$y_{3i} = \frac{e^{5(x_3-0.5-0.5i)} - e^{-5(x_3-0.5-0.5i)}}{e^{5(x_3-0.5-0.5i)} + e^{-5(x_3-0.5-0.5i)}}, \quad i = 1, 2, 3$$

$$y_{4i} = \frac{e^{5(x_4-0.5i)} - e^{-5(x_4-0.5i)}}{e^{5(x_4-0.5i)} + e^{-5(x_4-0.5i)}}, \quad i = 1, 2, 3$$

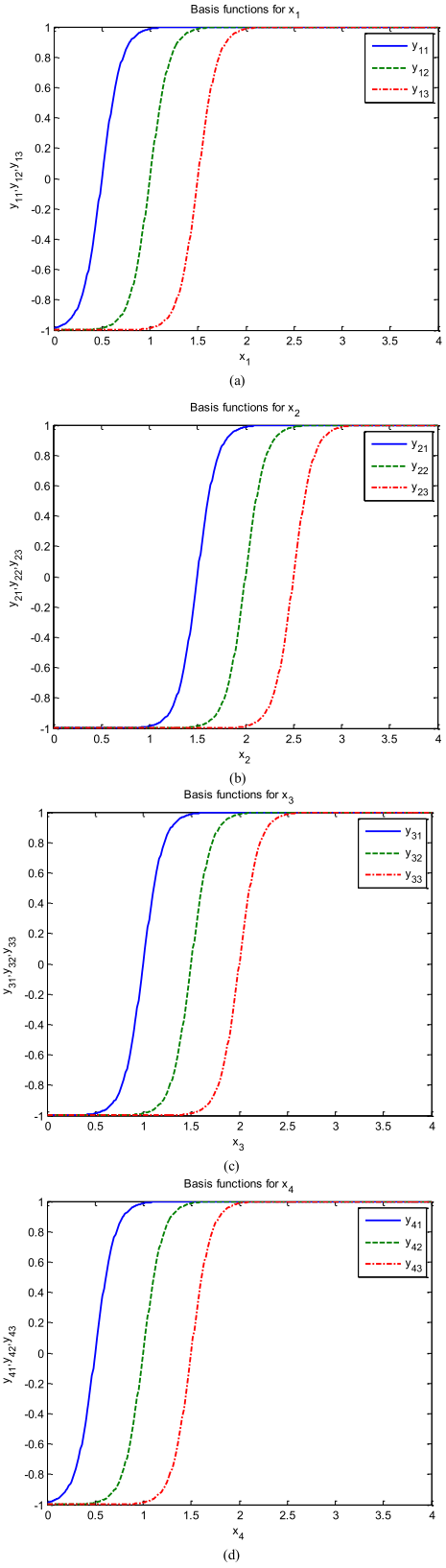

FIGURE 6. Activation functions of four input variables x_1, x_2, x_3, and x_4 in the neural network system. (a) The biases for x_1 are selected as 0.5, 1 and 1.5; (b) the biases for x_2 are selected as 1.5, 2 and 2.5; (c) the biases for x_3 are selected as 1, 1.5 and 2; (d) the biases for x_4 are selected as 0.5, 1 and 1.5.

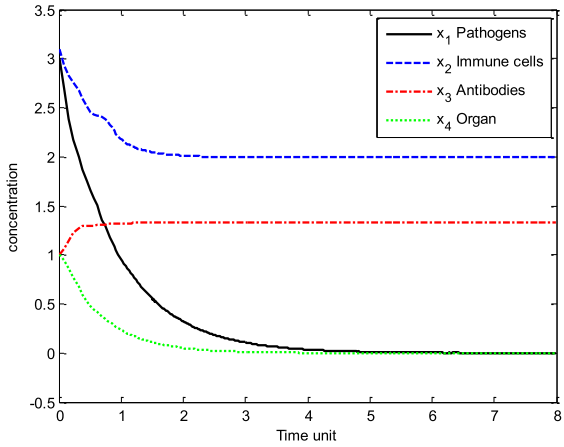

FIGURE 7. The response of the controlled innate immune system to the desired reference model by the robust adaptive neural network-based model matching control scheme with $x(0) = [3,\ 3.1,\ 1,\ 1]^T$.

Define $Y_1 = Y_2 = Y_3 = Y_4 = [y_{11}, y_{12}, y_{13}, \cdots, y_{41}, y_{42}, y_{43}]$. Hence, the neural network approximator $\hat{f}(x, \hat{\Theta}) = Y(x)\hat{\Theta}$ with $Y(x) = diag\{Y_1(x), Y_2(x), Y_3(x), Y_4(x)\}$, $\hat{\Theta} = [\hat{\theta}_1, \hat{\theta}_2, \cdots, \hat{\theta}_{47}, \hat{\theta}_{48}]^T$. Set the constrained region $\Omega_{\hat{\theta}} = R^{48}$. Three basis functions for each input are chosen, and the basis functions are shown in Fig. 6, respectively. The corresponding programs are provided in the Appendix C. Here, since the desired trajectory $x_{r1}(t)$ of the pathogen concentration $x_1(t)$ is positive and converges to zero as $t \to \infty$, it is intuitively evident that the biases of basis functions $y_{1i},\ i = 1, 2, 3$ should be clustered around zero and thus the biases are selected as 0.5, 1 and 1.5. Similarly, since the desired trajectory $x_{r2}(t)$ of the immune cell concentration $x_2(t)$ converges to 2 as $t \to \infty$, the biases of $y_{2i},\ i = 1, 2, 3$ should be clustered around 2 and thus the biases are selected as 1.5, 2 and 2.5. Since the desired trajectory $x_{r3}(t)$ of the antibody concentration $x_3(t)$ converges to 1.33 as $t \to \infty$, the biases of $y_{3i},\ i = 1, 2, 3$ should be clustered around 1.33 and thus the biases are selected as 1, 1.5 and 2. Finally, since the desired trajectory $x_{r4}(t)$ of the organ characteristic $x_4(t)$ is positive and converges to zero as $t \to \infty$, the biases of $y_{4i},\ i = 1, 2, 3$ should be clustered around 0 and thus the biases are selected as 0.5, 1 and 1.5. In general, the number of basis functions in the neural network system heavily influences the complexity of a neural network system. The larger the number, the more complex is the neural-network system and the higher the expected performance of the neural-network system.

Step 3: Give the desired attenuation level $\rho = 0.25$ and the weighting matrix $Q = I_{4\times4}$. In general, there is a tradeoff between the attenuation level and the amplitude of the control signal. The smaller ρ may yield better performance in attenuating the effect of the external disturbance on the model matching error, but the control signal during the transient time may be larger.

Step 4: Since $B_0 = diag\{-1, -1, 1, -1\}$ and $D = diag\{1, 1, 1, 1\}$, from assumption A1 set $\kappa_b = 0.2$. Solve the

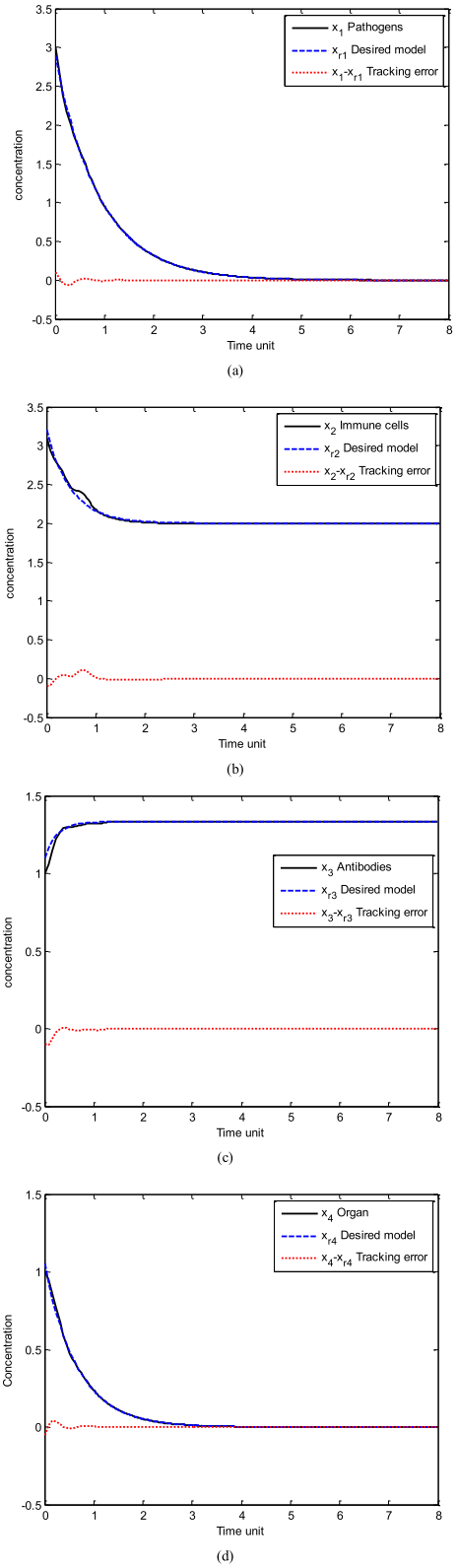

FIGURE 8. (a) The tracking responses of pathogen concentration x_1; (b) immune cell concentration x_2; (c) antibody concentration x_3; (d) organ characteristic x_4 in the controlled innate immune system with $x(0) = [3,\ 3.1,\ 1,\ 1]^T$ to match the desired reference model with $x_r(0) = [2.9,\ 3.2,\ 1.1,\ 1.05]^T$.

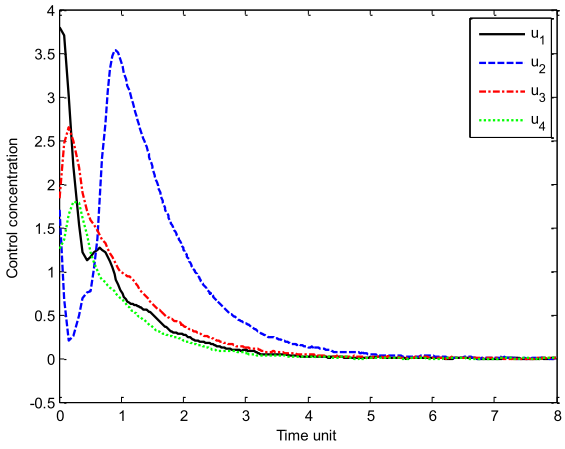

FIGURE 9. The control inputs in the controlled innate immune system by the robust adaptive neural network-based model matching control scheme.

inequality $(1/4\rho^2)DD^T - ((1-\kappa_b)/r_h)B_0B_0^T \le 0$ in (30). Therefore, the sufficient condition of the robust H_∞ control gain is $r_h \le 4\rho^2(1-\kappa_b) = 0.2$. Here, choose $r_h = 0.2$.

Step 5: Solve the inequality $PA_r + A_r^T P + 2Q \le 0$, and obtain the sufficient condition $PA_r \le -Q$. Since all the eigenvalues of the reference system matrix $A_r = diag\{-1.1, -2, -4, -1.5\}$ are less than -1 and the weighting matrix is $Q = I_{4\times4}$, we can simply choose $P = I_{4\times4}$.

Step 6: Construct the model matching controller (15)-(18) with $M_s = 0.1\,\|e\|$, $\varepsilon = 1$, $\nu = 0.1$, and $\gamma = 10$.

The response of the controlled innate immune system with $x(0) = [3,\ 3.1,\ 1,\ 1]^T$ and $\hat{\Theta}(0) = 0$ is presented in Fig. 7. The tracking responses of pathogen concentration x_1, immune cell concentration x_2, antibody concentration x_3, and organ characteristic x_4 are plotted in Figs. 8. The control inputs are presented in Fig. 9. The corresponding programs are provided in the Appendix D. Simulation results indicate that a satisfactorily tracking and convergent performance is achieved. Obviously, it can be found that after a short transient response all the pathogen, immune cell, and antibody concentrations, and organ characteristic can follow the desired reference trajectories with a small steady-state error. Consequently, the effects of the time-varying perturbations, the continuous intrusion of exogenous pathogens and the corruption of environmental disturbances have been compensated significantly by the proposed robust therapeutic control design.

Finally, in order to further demonstrate the effectiveness of the proposed control scheme, we make the following comparative simulations. From the lethal case of the uncontrolled innate immune response depicted in Fig. 5, it is clear that the pathogen concentration is increasing rapidly and causes organ failure. Now, we try to administrate a treatment after a period of pathogens infection to enhance the immune system. For the purpose of comparison, we simulate three comparative cases, that is, we take drugs at three time points 0.5, 1,

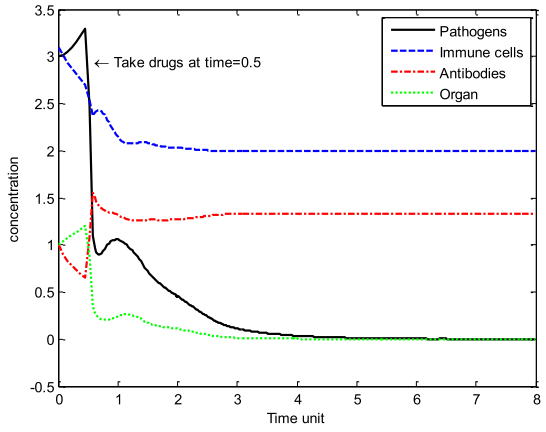

(a)

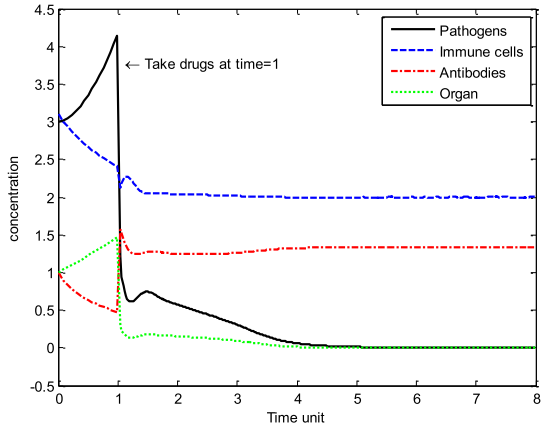

(b)

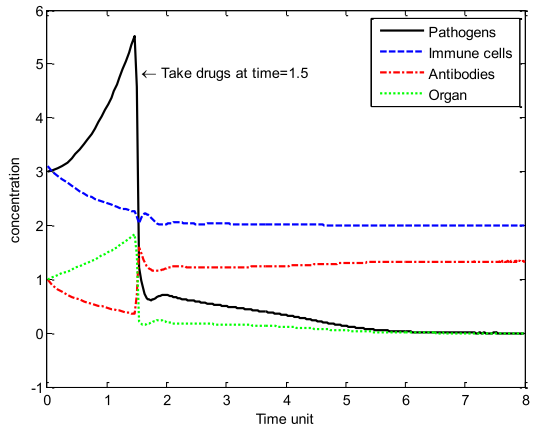

(c)

FIGURE 10. The response of the controlled innate immune system to the desired reference model by the robust adaptive neural network-based model matching control scheme. (a) The pathogens infect the immune system a period of time and the drugs are taken at time point 0.5; (b) The pathogens infect the immune system a period of time and the drugs are taken at time point 1; (c) The pathogens infect the immune system a period of time and the drugs are taken at time point 1.5.

and 1.5, respectively. The responses of the controlled innate immune system are presented in Fig. 10. Simulation results indicate that the pathogen concentration increases rapidly and causes organ failure at the beginning of the time period. Moreover, a satisfactorily tracking and convergent performance is achieved after the drugs are taken, showing that the pathogen concentration converges to zero and the organ becomes healthy.

V. CONCLUSION

An adaptive neural network-based model matching control design incorporated with a VSC algorithm and a nonlinear H_∞ control algorithm has been proposed and solved for a large class of uncertain nonlinear immune systems. All the states and signals of the closed-loop immune system are bounded and the model matching error can be made as small as possible. A simple and explicit solution of solving the modified algebraic Riccati-like inequality can also be exactly computed. Consequently, the intelligent robust control scheme developed here possesses the properties of computational simplicity and easy implementation from the viewpoint of practical applications. Finally, simulation examples are presented to demonstrate the effectiveness of the proposed robust therapeutic control design.

We assume in this study that all the state variables of immune systems are available for feedback. However, in reality the invading pathogens may migrate or hide in organs and therefore their concentration in the body is hard to measure. Moreover, in real biological systems some exact information of immune systems are not easily measured by biological monitoring techniques. Consequently, extended study of solving the adaptive observer-based model matching control without pathogen concentration measurement for uncertain nonlinear immune systems will be the subject of future research.

APPENDIX

A. PROGRAM OF SIMULATION FOR FIG 4

```
% file name: simu0.m
clear
t0=0;tf=8;x0=[3; 3.1; 1; 1];
options=odeset('RelTol',1e-4,'AbsTol',1e-5);
[t,x]=ode23('simup0',[t0,tf],x0,options);
plot(t,x(:,1),'k',t,x(:,2),'b–',t,x(:,3),'r-.',t,x(:,4),'g:')
axis([0 8 0 10])
% file name: simup0.m
% Subroutine of the program simu0.m
function xdot=simup0(t,x)
w1=0;w2=0;w3=0;w4=0;
u1=0;u2=0;u3=0;u4=0;
if x(4)>1/2;
   a21=0;
else
   a21=cos(pi*x(4));
end
xdot1=(1−x(3))*x(1)−u1+1*w1;
xdot2=a21*3*x(1)*x(3)−(x(2)−2)−u2+1*w2;
xdot3=x(2)−(1.5+x(1))*x(3)+u3+1*w3;
xdot4=0.5*x(1)-x(4)-u4+1*w4;
xdot=[xdot1;xdot2;xdot3;xdot4];
```

B. PROGRAM OF SIMULATION FOR FIG 5

```
% file name: xr.m
clear
t0=0;tf=10;x0=[2.9; 3.2; 1.1; 1.05];
options=odeset('RelTol',1e-4,'AbsTol',1e-5);
```

```
[t,x]=ode23('xrp',[t0,tf],x0,options);
plot(t,x(:,1),'k',t,x(:,2),'b–',t,x(:,3),'r-.',t,x(:,4),'g:')
% file name: xrp.m
% Subroutine of the program xr.m
function xdot=xrp(t,x)
Ar=[−1.1,0,0,0; 0,−2,0,0; 0,0,−4,0; 0,0,0,−1.5];
RR=[0;4;16/3;0];
xdot1=Ar*[x(1);x(2);x(3);x(4)]+RR;
xdot=xdot1;
```

C. PROGRAM OF SIMULATION FOR FIG 6

```
% file name: neural.m
% Program for Fig. 6a.
fplot('(exp(5*(x−0.5))-exp(-5*(x-0.5)))/(exp(5*…
(x-0.5))+exp(−5*(x-0.5)))',[0 4],'b');
hold on
fplot('(exp(5*(x−1))-exp(-5*(x-1)))/(exp(5*(x−1))+…
exp(−5*(x−1)))',[0 4],'g–');
fplot('(exp(5*(x−1.5))−exp(−5*(x−1.5)))/(exp(5*…
(x−1.5))+exp(−5*(x−1.5)))',[0 4],'r-.');
hold off
pause

% Program for Fig. 6b.
fplot('(exp(5*(x−1.5))−exp(−5*(x−1.5)))/(exp(5*…
(x−1.5))+exp(−5*(x−1.5)))',[0 4],'b');
hold on
fplot('(exp(5*(x−2))−exp(−5*(x−2)))/(exp(5*(x−2))+…
exp(−5*(x−2)))',[0 4],'g–');
fplot('(exp(5*(x−2.5))−exp(−5*(x−2.5)))/(exp(5*…
(x−2.5))+exp(−5*(x−2.5)))',[0 4],'r-.');
hold off
pause
% Program for Fig. 6c.
fplot('(exp(5*(x−1))−exp(−5*(x−1)))/(exp(5*(x−1))+…
exp(−5*(x−1)))',[0 4],'b');
hold on
fplot('(exp(5*(x−1.5))−exp(−5*(x−1.5)))/(exp(5*…
(x-1.5))+exp(-5*(x−1.5)))',[0 4],'g–');
fplot('(exp(5*(x−2))-exp(−5*(x−2)))/(exp(5*(x−2))+…
exp(−5*(x−2)))',[0 4],'r-.');
hold off
pause
% Program for Fig. 6d.
fplot('(exp(5*(x−0.5))−exp(−5*(x−0.5)))/(exp(5*…
(x−0.5))+exp(−5*(x−0.5)))',[0 4],'b');
hold on
fplot('(exp(5*(x−1))−exp(−5*(x−1)))/(exp(5*(x−1))+…
exp(−5*(x−1)))',[0 4],'g–');
fplot('(exp(5*(x−1.5))−exp(−5*(x−1.5)))/(exp(5*…
(x−1.5))+exp(−5*(x−1.5)))',[0 4],'r-.');
hold off
```

D. PROGRAM OF SIMULATION FOR FIGS 7-9

```
% file name: simu1.m
clear
t0=0;tf=8;int0=[0;0;0;0;0;0;0;0;0;0;0;0];
x0=[3; 3.1;1;1;2.9;3.2;1.1;1.05;int0;int0;int0;int0];
options=odeset('RelTol',1e−4,'AbsTol',1e−5);
[t,x]=ode23('simup1',[t0,tf],x0,options);
simuu1
% Program for Fig. 7.
plot(t,x(:,1),'k',t,x(:,2),'b–',t,x(:,3),'r-.',t,x(:,4),'g:')
pause
% Program for Fig. 8a.
plot(t,x(:,1),'k',t,x(:,5),'b–',t,x(:,1)-x(:,5),'r-.')
axis([0,8,-0.5,3.5])
pause
% Program for Fig. 8b.
plot(t,x(:,2),'k',t,x(:,6),'b–',t,x(:,2)−x(:,6),'r-.')
axis([0,8,−0.5,3.5])
pause
% Program for Fig. 8c.
plot(t,x(:,3),'k',t,x(:,7),'b–',t,x(:,3)−x(:,7),'r-.')
axis([0,8,−0.5,1.5])
pause
% Program for Fig. 8d.
plot(t,x(:,4),'k',t,x(:,8),'b–',t,x(:,4)−x(:,8),'r-.')
axis([0,8,−0.5,1.5])
pause
% Program for Fig. 9.
plot(t,u(1,:),'k',t,u(2,:),'b–',t,u(3,:),'r-.',t,u(4,:),'g:')
axis([0,8,−0.5,4])
% file name: simup1.m
% Subroutine 1 of the program simu1.m
function xdot=simup1(t,x)
% Regressor matrix
y11=(exp(5*(x(1)−0.5))−exp(5*(−x(1)+0.5)))/…
(exp(5*(x(1)−0.5))+exp(5*(−x(1)+0.5)));
y12=(exp(5*(x(1)−1))−exp(5*(−x(1)+1)))/…
(exp(5*(x(1)−1))+exp(5*(−x(1)+1)));
y13=(exp(5*(x(1)−1.5))−exp(5*(−x(1)+1.5)))/…
(exp(5*(x(1)−1.5))+exp(5*(−x(1)+1.5)));
y21=(exp(5*(x(2)−1.5))−exp(5*(−x(2)+1.5)))/…
(exp(5*(x(2)−1.5))+exp(5*(−x(2)+1.5)));
y22=(exp(5*(x(2)−2))−exp(5*(-x(2)+2)))/…
(exp(5*(x(2)−2))+exp(5*(−x(2)+2)));
y23=(exp(5*(x(2)−2.5))−exp(5*(−x(2)+2.5)))/…
(exp(5*(x(2)−2.5))+exp(5*(−x(2)+2.5)));
y31=(exp(5*(x(3)−1))−exp(5*(−x(3)+1)))/…
(exp(5*(x(3)−1))+exp(5*(−x(3)+1)));
y32=(exp(5*(x(3)−1.5))−exp(5*(−x(3)+1.5)))/…
(exp(5*(x(3)−1.5))+exp(5*(−x(3)+1.5)));
y33=(exp(5*(x(3)−2))−exp(5*(−x(3)+2)))/…
(exp(5*(x(3)−2))+exp(5*(-x(3)+2)));
y41=(exp(5*(x(4)−0.5))−exp(5*(−x(4)+0.5)))/…
(exp(5*(x(4)−0.5))+exp(5*(−x(4)+0.5)));
y42=(exp(5*(x(4)−1))−exp(5*(-x(4)+1)))/…
(exp(5*(x(4)−1))+exp(5*(−x(4)+1)));
y43=(exp(5*(x(4)−1.5))−exp(5*(−x(4)+1.5)))/…
(exp(5*(x(4)−1.5))+exp(5*(−x(4)+1.5)));
Y1=[y11 y12 y13 y21 y22 y23 y31 y32 y33 y41 y42 y43];
Y0=[0 0 0 0 0 0 0 0 0 0 0 0];
YY=[Y1 Y0 Y0 Y0;Y0 Y1 Y0 Y0;Y0 Y0 Y1 Y0;…
Y0 Y0 Y0 Y1];
Theta=[x(9) x(10) x(11) x(12) x(13) x(14) x(15) x(16)…
x(17) x(18) x(19) x(20) x(21) x(22) x(23) x(24) x(25)…
x(26) x(27) x(28) x(29) x(30) x(31) x(32) x(33) x(34)…
x(35) x(36) x(37) x(38) x(39) x(40) x(41) x(42) x(43)…
x(44) x(45) x(46) x(47) x(48) x(49) x(50) x(51) x(52)…
x(53) x(54) x(55) x(56)]';
% controller
e=[x(1)−x(5);x(2)−x(6);x(3)−x(7);x(4)−x(8)];
B=[−1,0,0,0; 0,−1,0,0; 0,0,1,0; 0,0,0,−1];
Ar=[−1.1,0,0,0; 0,−2,0,0; 0,0,−4,0; 0,0,0,−1.5];
RR=[0;4;16/3;0];
PP=[1,0,0,0; 0,1,0,0; 0,0,1,0; 0,0,0,1];
xx=[x(1);x(2);x(3);x(4)];
gamma=10; rgain=1/5;
uada=YY*Theta;
uh=-1/rgain*B'*PP*e;
Ms=0.1*sqrt(e'*e);
us=-B^(−1)*Ms/(1−0.2)*(Ms*B'*PP*e)/…
(sqrt((Ms*B'*PP*e)'*(Ms*B'*PP*e))+1*exp(−0.1*t));
u=inv(B)*(Ar*xx+RR-uada)+uh+us;
% system parameters
w=0.3*randn(4,1);
w1=w(1);w2=w(2);w3=w(3);w4=w(4);
if x(4)>1/2;
   a21=0;
else
   a21=cos(pi*x(4));
end
b1= −1+0.1*sin(t); b2= −1+0.1*cos(t);
b3=1+0.15*sin(t/2); b4= −1+0.12*cos(t/2);
u1=u(1);u2=u(2);u3=u(3);u4=u(4);
```

```
xdot1=(1−x(3))*x(1)+b1*u1+1*w1;
xdot2=a21*3*x(1)*x(3)−(x(2)−2)+b2*u2+1*w2;
xdot3=x(2)−(1.5+x(1))*x(3)+b3*u3+1*w3;
xdot4=0.5*x(1)−x(4)+b4*u4+1*w4;
xdot58=Ar*[x(5);x(6);x(7);x(8)]+RR;
thetadot=gamma*YY'*B'*PP*e;
xdot=[xdot1;xdot2;xdot3;xdot4;xdot58;thetadot];
% file name: simuu1.m
% Subroutine 2 of the program simu1.m
for i=1:max(size(t))
y11=(exp(5*(x(i,1)−0.5))−exp(5*(−x(i,1)+0.5)))/...
(exp(5*(x(i,1)−0.5))+exp(5*(−x(i,1)+0.5)));
y12=(exp(5*(x(i,1)−1))−exp(5*(−x(i,1)+1)))/...
(exp(5*(x(i,1)−1))+exp(5*(−x(i,1)+1)));
y13=(exp(5*(x(i,1)−1.5))−exp(5*(−x(i,1)+1.5)))/...
(exp(5*(x(i,1)−1.5))+exp(5*(−x(i,1)+1.5)));
y21=(exp(5*(x(i,2)−1.5))−exp(5*(−x(i,2)+1.5)))/...
(exp(5*(x(i,2)−1.5))+exp(5*(−x(i,2)+1.5)));

y22=(exp(5*(x(i,2)−2))−exp(5*(−x(i,2)+2)))/...
(exp(5*(x(i,2)−2))+exp(5*(−x(i,2)+2)));
y23=(exp(5*(x(i,2)-2.5))-exp(5*(−x(i,2)+2.5)))/...
(exp(5*(x(i,2)−2.5))+exp(5*(−x(i,2)+2.5)));
y31=(exp(5*(x(i,3)−1))−exp(5*(−x(i,3)+1)))/...
(exp(5*(x(i,3)−1))+exp(5*(−x(i,3)+1)));
y32=(exp(5*(x(i,3)−1.5))−exp(5*(−x(i,3)+1.5)))/...
(exp(5*(x(i,3)−1.5))+exp(5*(−x(i,3)+1.5)));
y33=(exp(5*(x(i,3)−2))−exp(5*(−x(i,3)+2)))/...
(exp(5*(x(i,3)−2))+exp(5*(−x(i,3)+2)));
y41=(exp(5*(x(i,4)−0.5))−exp(5*(−x(i,4)+0.5)))/...
(exp(5*(x(i,4)-0.5))+exp(5*(−x(i,4)+0.5)));
y42=(exp(5*(x(i,4)−1))−exp(5*(−x(i,4)+1)))/...
(exp(5*(x(i,4)−1))+exp(5*(−x(i,4)+1)));
y43=(exp(5*(x(i,4)−1.5))−exp(5*(−x(i,4)+1.5)))/...
(exp(5*(x(i,4)−1.5))+exp(5*(−x(i,4)+1.5)));
Y1=[y11 y12 y13 y21 y22 y23 y31 y32 y33 y41 y42 y43];
Y0=[0 0 0 0 0 0 0 0 0 0 0 0];
YY=[Y1 Y0 Y0 Y0;Y0 Y1 Y0 Y0;Y0 Y0 Y1 Y0;...
Y0 Y0 Y0 Y1];
Theta=[x(i,9) x(i,10) x(i,11) x(i,12) x(i,13) x(i,14)
x(i,15)...
x(i,16) x(i,17) x(i,18) x(i,19) x(i,20) x(i,21) x(i,22)...
x(i,23) x(i,24) x(i,25) x(i,26) x(i,27) x(i,28) x(i,29)...
x(i,30) x(i,31) x(i,32) x(i,33) x(i,34) x(i,35) x(i,36)...
x(i,37) x(i,38) x(i,39) x(i,40) x(i,41) x(i,42) x(i,43)...
x(i,44) x(i,45) x(i,46) x(i,47) x(i,48) x(i,49) x(i,50)...
x(i,51) x(i,52) x(i,53) x(i,54) x(i,55) x(i,56)]';
e=[x(i,1)−x(i,5);x(i,2)−x(i,6);x(i,3)−x(i,7);x(i,4)−x(i,8)];
B=[−1,0,0,0; 0,−1,0,0; 0,0,1,0; 0,0,0,−1];
Ar=[−1.1,0,0,0; 0,−2,0,0; 0,0,−4,0; 0,0,0,−1.5];
RR=[0;4;16/3;0];
PP=[1,0,0,0; 0,1,0,0; 0,0,1,0; 0,0,0,1];
xx=[x(i,1);x(i,2);x(i,3);x(i,4)];
rgain=1/5;
uada=YY*Theta;
uh=−1/rgain*B'*PP*e;
Ms=0.1*sqrt(e'*e);
us=−B^(−1)*Ms/(1-0.2)*(Ms*B'*PP*e)/...
(sqrt((Ms*B'*PP*e)'*(Ms*B'*PP*e))+1*exp(−0.1*i));
u(:,i)=inv(B)*(Ar*xx+RR−uada)+uh+us;
end
```

REFERENCES

[1] C. Janeway, *Immunobiology: The Immune System in Health and Disease*, Garland, NY, USA: Garland Science, 2005.

[2] M. Fribourg, B. Hartmann, M. Schmolke, N. Marjanovic, R. A. Albrecht, A. García-Sastre, S. C. Sealfon, C. Jayaprakash, and F. Hayot, "Model of influenza a virus infection: Dynamics of viral antagonism and innate immune response," *J. Theor. Biol.*, vol. 351, pp. 47–57, Jun. 2014.

[3] A. Hoshino, S. Hanada, N. Manabe, T. Nakayama, and K. Yamamoto, "Immune response induced by fluorescent nanocrystal quantum dots *in vitro* and *in vivo*," *IEEE Trans. Nanobiosci.*, vol. 8, no. 1, pp. 51–57, Mar. 2009.

[4] D. Milutinović and R. J. De Boer, "Process noise: An explanation for the fluctuations in the immune response during acute viral infection," *Biophys. J.*, vol. 92, no. 10, pp. 3358–3367, May 2007.

[5] R. F. Stengel, R. Ghigliazza, N. Kulkarni, and O. Laplace, "Optimal control of innate immune response," *Optim. Control Appl. Methods*, vol. 23, no. 2, pp. 91–104, 2002.

[6] R. F. Stengel and R. Ghigliazza, "Stochastic optimal therapy for enhanced immune response," *Math. Biosci.*, vol. 191, no. 2, pp. 123–142, Oct. 2004.

[7] W. H. Kim, H. B. Chung, and C. C. Chung, "Optimal switching in structured treatment interruption for HIV therapy," *Asian J. Control*, vol. 8, no. 3, pp. 290–296, Oct. 2008.

[8] W. M. Haddad, J. M. Bailey, B. Gholami, and A. R. Tannenbaum, "Clinical decision support and closed-loop control for intensive care unit sedation," *Asian J. Control*, vol. 15, no. 2, pp. 317–339, 2013.

[9] R. Medzhitov, "Recognition of microorganisms and activation of the immune response," *Nature*, vol. 449, no. 7164, pp. 819–826, Oct. 2007.

[10] G.-B. Stan, R. Fonteneau, C. Michelet, F. Zeggwagh, F. Belmudes, D. Ernst, and M.-A. Lefebvre, "Modelling the influence of activation-induced apoptosis of $CD4^+$ and $CD8^+$ T-cells on the immune system response of a HIV-infected patient," *IET Syst. Biol.*, vol. 2, no. 2, pp. 94–102, Mar. 2008.

[11] C. F. Arias, M. A. Herrero, F. J. Acosta, and C. Fernandez-Arias, "A mathematical model for a T cell fate decision algorithm during immune response," *J. Theor. Biol.*, vol. 349, pp. 109–120, May 2014.

[12] Y. Su, L. Zhao, and L. Min, "Analysis and simulation of an adefovir anti-hepatitis b virus infection therapy immune model with alanine aminotransferase," *IET Syst. Biol.*, vol. 7, no. 5, pp. 205–213, Oct. 2013.

[13] W. Zhang and X. Zou, "Systematic analysis of the mechanisms of virus-triggered type I IFN signaling pathways through mathematical modeling," *IEEE/ACM Trans. Comput. Biol. Bioinf.*, vol. 10, no. 3, pp. 771–779, May 2013.

[14] H. Chang and A. Astolfi, "Activation of immune response in disease dynamics via controlled drug scheduling," *IEEE Trans. Autom. Sci. Eng.*, vol. 6, no. 2, pp. 248–255, Apr. 2009.

[15] T.-L. Chien, C.-C. Chen, and C.-J. Huang, "Feedback linearization control and its application to MIMO cancer immunotherapy," *IEEE Trans. Control Syst. Technol.*, vol. 18, no. 4, pp. 953–961, Jul. 2010.

[16] H. Jiao, Q. Shen, Y. Shi, and P. Shi, "Adaptive tracking control for uncertain cancer-tumor-immune systems," *IEEE/ACM Trans. Comput. Biol. Bioinf.*, vol. 18, no. 6, pp. 2753–2758, Nov. 2021, doi: 10.1109/TCBB.2020.3036069.

[17] M. Sharifi, A. A. Jamshidi, and N. N. Sarvestani, "An adaptive robust control strategy in a cancer tumor-immune system under uncertainties," *IEEE/ACM Trans. Comput. Biol. Bioinf.*, vol. 16, no. 3, pp. 865–873, May 2019.

[18] F. Dai and B. Liu, "Optimal control problem for a general reaction–diffusion tumor–immune system with chemotherapy," *J. Franklin Inst.*, vol. 358, no. 1, pp. 448–473, Jan. 2021.

[19] H. S. Wong and R. N. Germain, "Robust control of the adaptive immune system," *Seminars Immunol.*, vol. 36, pp. 17–27, Apr. 2018.

[20] M. M. McDaniel, H. E. Meibers, and C. Pasare, "Innate control of adaptive immunity and adaptive instruction of innate immunity: Bi-directional flow of information," *Current Opinion Immunol.*, vol. 73, pp. 25–33, Dec. 2021.

[21] J. O. Abaricia, N. Farzad, T. J. Heath, J. Simmons, L. Morandini, and R. Olivares-Navarrete, "Control of innate immune response by biomaterial surface topography, energy, and stiffness," *Acta Biomaterialia*, vol. 133, pp. 58–73, Oct. 2021.

[22] F. Heiran, J. Khodaei-Mehr, R. Vatankhah, and M. Sharifi, "Nonlinear adaptive control of immune response of renal transplant recipients in the presence of uncertainties," *Biomed. Signal Process. Control*, vol. 63, Jan. 2021, Art. no. 102163.

[23] J. A. Farrell and M. M. Polycarpou, *Adaptive Approximation Based Control: Unifying Neural, Fuzzy and Traditional Adaptive Approximation Approaches*. Hoboken, NJ, USA: Wiley, 2006.

[24] Z. Chen, F. Huang, W. Sun, J. Gu, and B. Yao, "RBF-neural-network-based adaptive robust control for nonlinear bilateral teleoperation manipulators with uncertainty and time delay," *IEEE/ASME Trans. Mechatronics*, vol. 25, no. 2, pp. 906–918, Apr. 2020.

[25] M. Moghtadaei, M. R. H. Golpayegani, and R. Malekzadeh, "A variable structure fuzzy neural network model of squamous dysplasia and esophageal squamous cell carcinoma based on a global chaotic optimization algorithm," *J. Theor. Biol.*, vol. 318, pp. 164–172, Feb. 2013.

[26] J. Khodaei-Mehr, S. Tangestanizadeh, R. Vatankhah, and M. Sharifi, "Optimal neuro-fuzzy control of hepatitis C virus integrated by genetic algorithm," *IET Syst. Biol.*, vol. 12, no. 4, pp. 154–161, Aug. 2018.
[27] B.-S. Chen, C.-H. Chang, and Y.-J. Chuang, "Robust model matching control of immune systems under environmental disturbances: Dynamic game approach," *J. Theor. Biol.*, vol. 253, no. 4, pp. 824–837, Aug. 2008.
[28] B.-S. Chen, Y.-P. Lin, and Y.-J. Chuang, "Robust H∞ observer-based tracking control of stochastic immune systems under environmental disturbances and measurement noises," *Asian J. Control*, vol. 13, no. 5, pp. 667–690, Sep. 2011.
[29] Y.-C. Chang, "Intelligent robust tracking control for a class of uncertain strict-feedback nonlinear systems," *IEEE Trans. Syst. Man, Cybern. B, Cybern.*, vol. 39, no. 1, pp. 142–155, Feb. 2009.
[30] A. Asachenkov, G. Marchuk, R. Mohler, and S. Zuev, *Disease Dynamics*. Boston, MA, USA: Birkhauser, 1994.
[31] H. K. Khalil, *Nonlinear Systems*, 3rd ed. Upper Saddle River, NJ, USA: Prentice-Hall, 2002.

YEONG-CHAN CHANG was born in Tainan, Taiwan. He received the M.S. and Ph.D. degrees in electrical engineering from the National Tsing Hua University, in 1991 and 1995, respectively. Since 2000, he has been a Professor with the Department of Electrical Engineering, Kun-Shan University, Tainan. His current research interests include nonlinear control, adaptive control, intelligent control, constrained mechanical systems, and signal processing.

HUI-MIN YEN received the B.S. and M.S. degrees in electrical engineering from Kun Shan University, Tainan, Taiwan, in 1999 and 2003, respectively, and the Ph.D. degree in electrical engineering from the National Cheng Kung University, Tainan, in 2012. He is currently an Assistant Research Fellow with the Green Energy Technology Research Center, Kun Shan University. His current research interests include non linear control, adaptive control, and intelligent control.

KUANG-FEN HAN was born in Taichung, Taiwan. She received the M.S. degree from the Graduate Institute of Pharmacology, National Defense Medical Center, in 1996. She has been a Lecturer with the Department of Nursing, Min-Hwei Junior College of Health Care Management, Tainan, Taiwan, since 1998. Her current research interests include medicine theory and immune systems.